

# A Mixed-Signal VLSI System for Producing Temporally Adapting Intraspinal Microstimulation Patterns for Locomotion

Kevin A. Mazurek, *Member, IEEE*, Bradley J. Holinski, Dirk G. Everaert, Vivian K. Mushahwar, *Member, IEEE*, and Ralph Etienne-Cummings, *Fellow, IEEE*

**Abstract**—Neural pathways can be artificially activated through the use of electrical stimulation. For individuals with a spinal cord injury, intraspinal microstimulation, using electrical currents on the order of  $125 \mu\text{A}$ , can produce muscle contractions and joint torques in the lower extremities suitable for restoring walking. The work presented here demonstrates an integrated circuit implementing a state-based control strategy where sensory feedback and intrinsic feed forward control shape the stimulation waveforms produced on-chip. Fabricated in a  $0.5 \mu\text{m}$  process, the device was successfully used *in vivo* to produce walking movements in a model of spinal cord injury. This work represents progress towards an implantable solution to be used for restoring walking in individuals with spinal cord injuries.

**Index Terms**—Central pattern generator (CPG), intraspinal microstimulation, locomotion, mixed signal VLSI, neural prostheses, neural stimulation.

## I. INTRODUCTION

HERE have been significant advancements in the design and performance of neural prostheses which restore neural function in recent years [1]–[4]. Techniques such as intraspinal microstimulation (ISMS), intracortical microstimulation (ICMS) and optogenetics have introduced novel methods for eliciting neural activity [5]–[14]. These techniques possess the capabilities to activate remaining neural pathways for restoring motor control to individuals with lost or impaired function.

In the United States, approximately 12 000 new cases of spinal cord injury (SCI) occur each year [15]. The resulting

Manuscript received May 06, 2015; revised July 24, 2015 and September 18, 2015; accepted October 25, 2015. Date of publication March 09, 2016; date of current version July 26, 2016. K. A. Mazurek was supported by NIH-NINDS under award F31NS074828 and V. K. Mushahwar was supported by NIH-NINDS NS44225, Canadian Institutes of Health Research, and Alberta Innovates-Health Solutions (AIHS). This paper was recommended by Associate Editor S.-C. Liu.

K. A. Mazurek and R. Etienne-Cummings are with the Electrical and Computer Engineering Department, Johns Hopkins University, Baltimore, MD 21218 USA (e-mail: kmazurek@jhu.edu).

B. J. Holinski is with the Biomedical Engineering Department, University of Alberta, Edmonton, AB T6G 2R3, Canada.

D. G. Everaert is with the Physiology Department, University of Alberta, Edmonton, AB T6G 2R3, Canada.

V. K. Mushahwar is with the Physical Medicine and Rehabilitation Department, University of Alberta, Edmonton, AB T6G 2R3, Canada.

Color versions of one or more of the figures in this paper are available online at <http://ieeexplore.ieee.org>.

Digital Object Identifier 10.1109/TBCAS.2015.2501419

loss of mobility causes a dramatic increase in the physical effort required to perform daily tasks and severely affects an individual's quality of life. A neural prosthesis for restoring locomotion must simultaneously control multiple joints in the lower extremities to ensure proper force production and limb movement. The two main approaches, exoskeletal systems and functional electrical stimulation (FES), have had varying levels of success with functional improvement dependent on the severity of the injury [16]–[23]. For example, an individual with an incomplete SCI may have limited neural communication to their lower limbs and may benefit from an assistive FES device which augments the existing function [16]–[18]. An individual with a complete SCI will have minimal-to-no neural communication and requires a device such as a walking exoskeleton to provide trunk support and motor control [19]–[21].

When electrically stimulating muscles, the distance the individual can walk is directly correlated to the fatigability of the target muscles and the muscle's ability to produce controlled force. If the muscles fatigue quickly, the individual would need to rest after walking short distances until the muscles recover. By targeting fatigue resistant muscle fibers, walking movements and forces can be produced over longer durations before the individual must rest and recover. ISMS is one solution for activating muscles in such a manner, as the elicited movements tend to be fatigue resistant since the slow-twitch fibers are recruited first in a biofidelic manner [8], [11]. ISMS electrically activates neural pathways in the spinal cord to produce forces and movements adequate for walking [5]–[8], [11], [14]. Microwires ( $\leq 50 \mu\text{m}$  diameter) are inserted into the ventral horn of the spinal cord, which electrically activate lower limb muscles with low stimulation currents ( $\leq 125 \mu\text{A}$ ) [14]. Other peripheral nerve stimulation methods require much greater stimulation amplitudes. Levy *et al.* demonstrated that using surface electrodes to activate quadriceps muscles require up to 220 mA [24]. Intramuscular stimulation (IMS) activates motor neurons which innervate the target muscles, where 20–50 mA stimulation amplitudes can produce walking forces and movements [25]. This is comparable to the stimulation involved in intracortical microstimulation [26]–[30]. This low ISMS current amplitude is advantageous for designing a low power, integrated system to produce and control walking movements.

A suitable control strategy is also required to coordinate these multi-joint movements. Previous work utilized IF-THEN rules in a state-space control strategy to produce over-ground walking

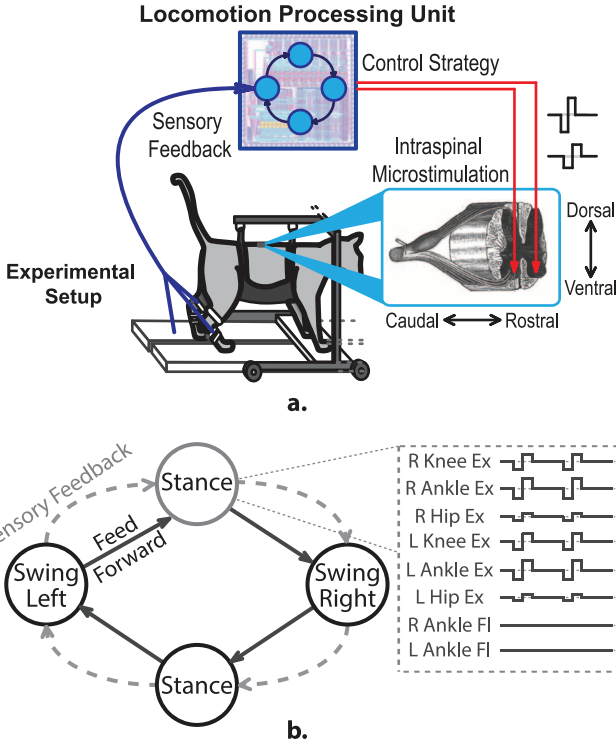


Fig. 1. (a) Experimental setup integrating the LPU to produce intraspinal microstimulation patterns. (b) A depiction of a 4 state walking cycle where transitions occur by either sensory feedback or intrinsic feed forward control. Stimulation amplitudes in each state activate flexion (Fl) or extension (Ex) movements in the lower limbs. The amplitude of stimulation is dependent on the placement of the ISMS electrode which affects the threshold voltage for producing movements. A subset of channels during the Stance state are shown for the hips, knees, and ankles activity.

in a cat model of SCI [31], [32]. Other work has demonstrated that neuromorphic silicon neurons can produce patterned movements with spiking outputs comparable to the biological locomotion central pattern generator (CPG) [33]. The combination of open and closed-loop control ensures safe transitions between swing and stance with proper supportive force as shown during *in vivo* experiments and in simulations [31]–[35]. Such a control strategy can be implemented in a system-on-chip as the central processor to a walking prosthesis.

The results presented in this manuscript are from a prototype walking prosthesis capable of producing temporally changing ISMS waveforms for restoring locomotion. A generalized version of the control strategy previously used by Mazurek *et al.* which restored walking *in vivo* using IMS [32] has been implemented on chip to be used with an ISMS system. Preliminary results from this experimental setup have demonstrated successful restoration of stepping in a cat model of spinal cord injury [14]. The mixed signal VLSI integrated circuit (IC) in this work is called a locomotion processing unit (LPU) and contains ISMS current outputs, programmable control logic, and sensory feedback (some of which has been previously described [36], [37]). The first version prototype LPU demonstrated successful *in vivo* walking results using ISMS and the implemented control strategy in an experimental setup similar to that depicted in Fig. 1(a). The rest of this manuscript describes the functionality of the hardware in greater detail.

## II. LPU ARCHITECTURE

As previously demonstrated using intramuscular stimulation (IMS), integration of external sensory feedback (from accelerometers, gyroscopes, force plates) and intrinsic feed forward control produced stable, coordinated movements across the joints of the lower extremities during bipedal locomotion in an anesthetized cat model. The proposed LPU contains the necessary architecture to program different patterns of stimulation as shaped by feedback and feed forward control signals. This architecture consists of three different functional components that are described in the following Sections (II.A–II.C) along with their implementation in CMOS circuitry. This control strategy is a generalized version of the strategy which produced *in vivo* walking results using IMS and using ISMS as described in Section II.D.

### A. Control Logic

The control logic implemented a state-space control strategy which adjusted the stimulation output based on the programmed state-space connectivity. A state-based approach mapped different functional movements of the biological walking cycle to specific states in the LPU control logic. This allowed for realizing different synergistic movements (co-ordinated multi-joint movements) in each state (e.g., swing, stance, and push-off). The cat step cycle is classically divided into four phases of functional movement [38]–[40]. LPU control logic states were programmed to activate joint flexors or extensors in order to produce the function movements in each of these classical walking phases. This required specifying which muscles would be active in each state and the amplitude of activation. Once the desired muscle activations in each state in the LPU was defined, transitions between states were programmed to produce the walking pattern, thus temporally shaping the stimulation waveform. A cartoon depiction of such a state-based controller is shown in Fig. 1(b), representing a simplified walking pattern. ISMS electrodes can have different threshold levels to elicit movements, and this is reflected in the different stimulation amplitudes depicted in the cartoon representation.

The control logic utilized parameters in the LPU that were necessary to realize a desired control strategy. These parameters are listed in Table I and were programmed for each state of the LPU. These parameters were associated with a functional component of the LPU architecture. For the sensory rules, parameters included selecting external sensory input signals, rule logic voltage thresholds, and the logic function realized by the rule (described in Section II.B). An additional timing rule executed the feed forward control and allowed a state transition to occur after a defined duration. Each rule was programmed to point to the destination states to be implemented for the complete walking control strategy. A depiction of how the states transition during operation is described in Fig. 2. Programmable stimulation properties included the pulse width, frequency, amplitudes (anodic and cathodic), waveshape (monophasic, biphasic, anodic leading, cathodic leading), and enabling the channel (described in Section II.C).

Custom operational codes (OPcodes) were developed for programming these parameters in the LPU. The available resources to the LPU (e.g., number of states, stimulation outputs,

TABLE I  
OPCODE PARAMETERS

Functional Component	Parameter Name	Parameter Subtype
Control Logic	Destination States	<i>Sensory Rules</i> <i>Timing Rule</i>
Transition Rules	Sensory Rules	Voltage threshold Sensory input signals Rule Solution <i>Enable Rule</i>
		<i>Threshold</i>
Stimulation Output	Timing Rule	<i>Anodic</i> <i>Cathodic</i>
	Amplitude	
	Frequency	
	Pulse Width	
<i>Enable Channel</i>		

*Italics parameters:* implemented on chip, adjusted on a state-by-state basis

TABLE II  
LPU PARAMETERS

Parameter	0.5μm Version
Vdd	5V (+/-2.5V)
Capacitors	Poly over poly
Sensory Rules	8
Comparators per rule	4
Voltage DAC	8 bit
Stimulation Channels	14
Stimulation Resolution bits	12
Waveshape	6 programmable shapes
Communication Interface	Parallel I/O
SRAM	External
Programmable States	128
Opcode bit length	16

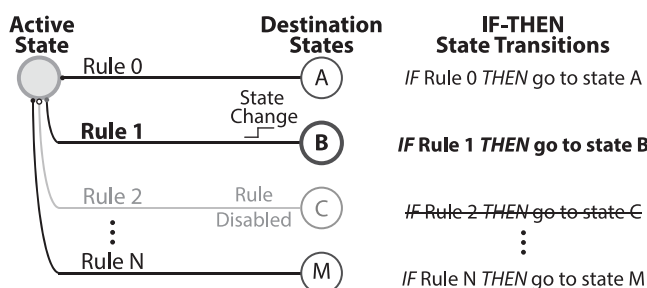


Fig. 2. The active state contains programmable connections to several destination states. In the above example, Rule 1 activates the transition from the Active State to State B. It is possible to disable any of the rules (such as Rule 2) and by programming the different destination states for all states in use it creates a complete connectivity matrix for the algorithm. The number of rules is generalized as  $N$  and total states as  $M$ . These values are typically constrained by the amount of resources available in the system (e.g., memory size on chip, number of sensory signals).

or sensory rules) determined the minimum bit length of the OPcodes. The least significant bits (LSBs) of the OPcodes encoded the applicable state for state-dependent parameters of the LPU. For state-independent parameters, these LSB values were “don’t cares.” The most significant bits (MSBs) of the

OPcode specified which parameter value was being read or written.

SRAM cells stored the parameter values where the memory address was accessed via a parallel bus and each parallel memory address matched an LPU Opcode. The parameter values were also loaded into on-chip registers used by the active state during operation (e.g., transition rule execution, stimulation output). These registers updated from the SRAM upon each state transition.

### B. State Transition Rules

The state transitions controlled by the OPcodes described in Section II.A occurred using on-chip rule logic. These rules consisted of one temporal transition rule along with a set of sensory-based rules. This allowed for realizing feed forward control (also called intrinsic or open-loop control) in addition to feedback control (closed loop). When an enabled rule evaluated true, it signaled to the control logic to update the LPU parameters to the new active state. The designed logic structure realized several forms of “IF-THEN” rules based on the success of previous *in vivo* walking experiments.

A block diagram of one individual rule is shown in Fig. 3. Each sensory rule contained a set of analog comparators where external analog signals are selected as inputs to the positive terminal. The negative terminal input for each comparator was a programmable threshold in the form of a capacitive voltage digital to analog converter (DAC). These analog comparators yielded a decoded digital output realizing a set of logic functions. In the general case of  $B$  comparators, the number of realized functions is  $2^B$ . The decoded output was bitwise compared to a programmed rule solution parameter. If any of the bitwise pairs realized a logic AND, the rule evaluated as true and signaled to the control logic to implement a state change. Additionally, each sensory rule could be enabled or disabled during each state.

For the timing rule, a counter with the same bit length as the timing threshold parameter was bitwise compared to determine when the rule evaluated TRUE. The counter clock frequency determined the longest duration for which a timing rule could evaluate.

Since all of the rules (sensory and timing) operated in parallel, priority levels were hardcoded if multiple rules evaluated TRUE simultaneously. The sensory rules were given priority over the timing rule to modulate the output stimulation similar to how spinal reflexes quickly modulate the biological CPG. These rules establish the state-space which shapes the stimulation output waveforms for the desired step cycle.

### C. Stimulation Output

The output stage for each state produced programmable current stimulation waveforms connected to neural electrodes to activate different leg muscles (Fig. 4). Stimulation shapes for FES applications included: monophasic or biphasic; symmetric or asymmetric; and anodic or cathodic pulses. The first stage of the stimulus circuitry used an integrate and fire neuron to generate the current output. While a programmable oscillator could have been implemented instead of the integrate and fire neuron circuit, the design of the LPU was intended to have

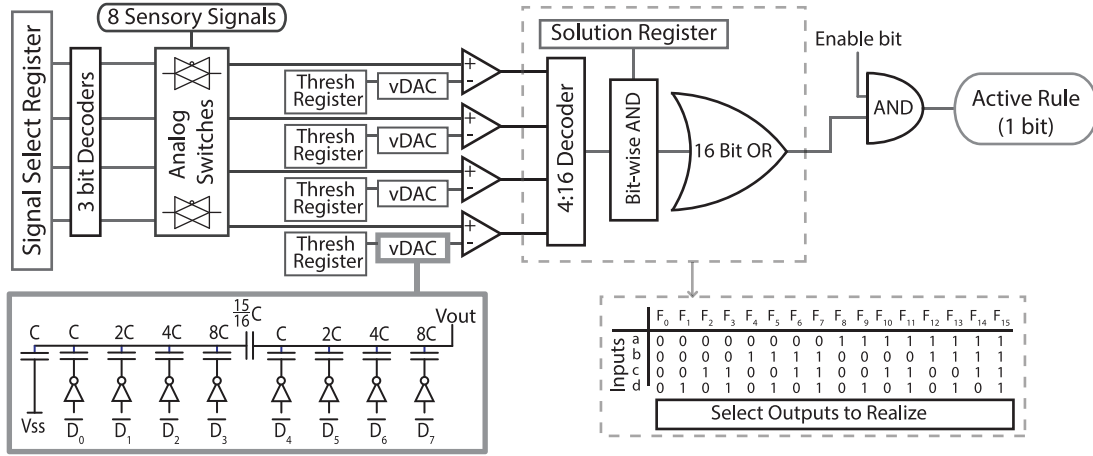


Fig. 3. This block level depiction of the sensory rule shows the analog inputs, the voltage DACs for each comparator, and the comparison of the digital output to a programmed value. In this depiction, the number of binary comparators is four allowing for 16 different output functions to be realized (dashed box). A total of 8 sensory signals could be selected from as inputs to the comparators.

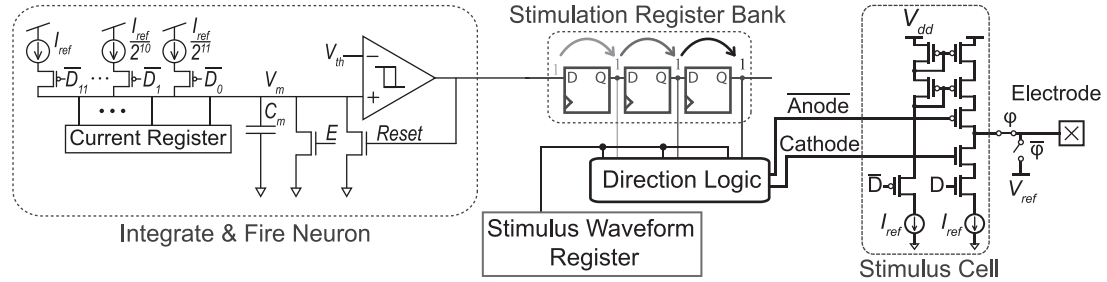


Fig. 4. A block diagram of the stimulation circuits. The integrate and fire neuron loads a ‘1’ into the register bank. This propagates through the bank where each location activates either an anodic, cathodic or no current. The anodic signal is inverted to activate the PMOS cascaded current mirror. The data signal is from the digital value to control the amplitude and the reference current sources shown are from split mirrors of the current bias reference circuit.

the ability to translate into a neuromorphic design in future iterations. This would allow for the use of more detailed silicon neuron models or networks, and this implementation of the integrate and fire neuron would serve as a starting point for such a design.

For each output channel, a programmable, digital weight applied current to the integrate and fire neuron membrane capacitor via a current mode DAC. This current set the rate at which the neuron would fire, subsequently setting the stimulation frequency. When the membrane voltage exceeded a globally set threshold voltage, a digital output “spike” was produced, setting an SR latch. This loaded a logic ‘1’ into a shift register bank which propagated through to apply cathodic or anodic current on the output electrode. The number of shift registers in the bank and the stimulation clock frequency defined the total stimulation duration.

A bias current reference circuit was split and mirrored to each stimulation output slice [41]. This bias reference circuit was used due to its small layout area and low power requirements. A digital weight programmed these split current mirrors to be connected to the output electrode. For anodic current, the mirror cascaded through PMOS transistors while cathodic current cascaded through NMOS transistors. Each transistor was sized during simulation to provide accurate current matching, however fabrication mismatch still caused variability in the programmable output levels. Charge balancing switches connected

the output electrode to either the current output node or a reference voltage ( $V_{ref}$ ) to prevent charge buildup and damage to the neural tissue. Programming different anodic and cathodic current weights for each wave shape allowed for adjusting potential mismatch between NFETs and PFETs during fabrication.

#### D. In Vivo Application

The 0.5  $\mu$ m LPU was used in an *in vivo* experiment where ISMS was applied to the lumbosacral region in the spinal cord of an anesthetized cat to produce walking across an instrumented walkway. All experimental procedures were approved by the University of Alberta’s Animal Care and Use Committee. This was the same procedure as implemented in previous ISMS experiments [14]. The cat was anesthetized with sodium pentobarbital and a laminectomy was performed on vertebrae L4 to L6 to expose spinal cord segments L4-S1. A custom microwire array (Pt-Ir 80–20%, 50  $\mu$ m diameter, 100  $\mu$ m de-insulated tip) was implanted bilaterally with 12 electrodes per side. Hip, knee, and ankle flexors and extensors and a full limb extensor synergy were targeted for each side based on previous maps of motor neuron pools [42]–[46]. A reference electrode (nine-strand stainless-steel wire, Teflon insulated, 5 cm end bared) was placed over the longissimus dorsi muscle [42], [46]. After implantation, the cats were transferred to an instrumented 2.9 m walkway and partially suspended in a cart-mounted sling and maintained under anesthesia. Motion

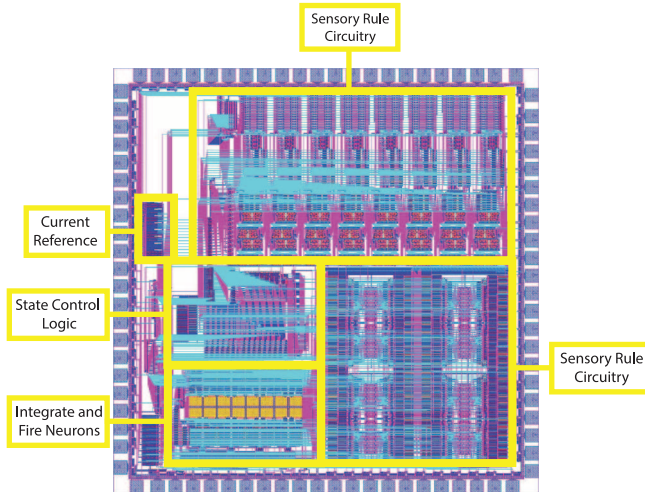


Fig. 5. Integrated circuit fabrication layout.

tracking markers were fixed to the right hind limb to record kinematics with a camcorder positioned 4.5 m away from the midpoint of the walkway with lens parallel to the walkway (120 fps, JVC Americas Corp., Wayne, NJ, USA). Markers were placed on the iliac crest, hip, knee, ankle and metatarsophalangeal joints. Force transducers mounted under the walkway plates captured independent left and right supportive (vertical) and propulsive (horizontal) forces. Accelerometers and gyroscopes were affixed to the hind limbs to estimate limb angle and were used as external sensors to the LPU to provide feedback. The LPU stimulation output consisted of a monopolar, cathodic-leading biphasic stimulation pattern (pulse width 245  $\mu$ s) at approximately 60 Hz using 14 different output channels.

### III. INTEGRATED CIRCUIT DESIGN

The architecture described in Section II has been implemented in the ON Semi 0.5  $\mu$ m process and the layout is depicted in Fig. 5. This IC provided a proof-of-concept to the performance of the architecture. It was designed with a 16-bit instruction bus width for the OPcodes and parameter values. The I/O of the control logic was programmed in parallel and an external SRAM chip (IDT71016S, IDT 1 MB SRAM) also addressed in parallel stored the LPU parameters using the hardcoded OPcodes. The stimulation output contained 6 programmable shapes as previously described [36], [37]. These outputs were programmable with the same digital value setting the anodic and cathodic currents. Separate anodic and cathodic programmable weights were not included in this iteration due to size constraints. Off-chip analog switches (ADG1234, Analog Devices iCMOS Switch) were used to connect and disconnect the electrode to the LPU stimulating output and ensure proper charge balancing.

A prototype board included a microcontroller (dsPIC30F6014A, Microchip) to program the LPU and off-chip components, as well as to record external sensor data during operation. The intended application of this device was to demonstrate its ability to produce walking movements and forces in an anesthetized cat using ISMS [14]. The device needed to deliver current levels up to 125  $\mu$ A over a 20 k $\Omega$

electrode load [14]. The chip was powered to  $\pm 2.5$  V to bias the current outputs around 0 V. Again due to on-chip space limitations, 14 stimulation channels were included as outputs compared to the 16 channels used in the external hardware setup for producing over-ground walking with ISMS [14]. On-chip poly-over-poly capacitors were used for the split capacitor voltage DAC in the sensory rule thresholds and integrate and fire neuron membrane capacitors (5 pf). Eight sensory rules were included on-chip with an additional timing rule for feed forward control. The device was capable of programming up to 128 states, although for the *in vivo* cat experiments nine of these states were actually used [14], [32]. These experiments used external sensors in the forms of gyroscopes, accelerometers, and force plates to transition between states of the walking cycle. Average hip, knee, and ankle angular excursions produced by this controller using sensory feedback were 24, 39, and 68 degrees, respectively [32]. The LPU system was designed to operate using similar external sensory signals. Custom software written in MATLAB (Mathworks, Inc. Natick, MA, USA) was used to program the device through a USB-to-RS232 connection (FT232R, FTDI).

### IV. RESULTS

The target application for the fabricated circuit was to produce stimulating currents for an ISMS array with an estimated output impedance of 20 k $\Omega$  [14]. The average current sweeps from all 14 output channels over a short circuit load (0  $\Omega$ ) and a 20 k $\Omega$  resistor are depicted in Fig. 6. The input codes were calibrated off-chip such that the cathodic current changed monotonically. In Fig. 6(a), the current output could reach 500  $\mu$ A when the voltage compliance is not reached (as in the 0  $\Omega$  measurements). However, in the 20 k $\Omega$  measurements, the voltage compliance reduced the effective operating range. Fig. 6(b) depicts an expanded region of input codes (0–1024) along with the differential current amplitude between the cathodic and anodic currents. It is evident that at the higher input codes when the voltage compliance takes effect the current mismatch spikes to upwards of 5  $\mu$ A. Fabrication mismatch between the NMOS and PMOS transistor thresholds may also contribute to this fluctuation in current mismatch. Based on the results shown by Cogan, microelectrodes can safely perform with a charge per phase threshold of 2 nC per phase [47]. Using these DC measurements with a phase duration of 245  $\mu$ s, a maximum allowed current mismatch of 8.16  $\mu$ A (2 nC/245  $\mu$ s) should not yield histological damage. However, verifying using histology after *in vivo* stimulation would provide additional and useful insight into how accurate an estimation this is. Fig. 7 depicts the performance during an *in vivo* experiment and the resulting ground reaction forces (GRFs) from one trial. Fig. 7(a) shows an open loop stimulation pattern similar to that used during the *in vivo* experiment. Each row corresponds to the temporal stimulation of an ISMS electrode channel. These measurements were taken over a 20 k $\Omega$  resistor to estimate the impedance of the ISMS electrode array.

The results of these trials using the LPU were a subset of a larger study demonstrating the efficacy of ISMS for producing walking for long distances and durations using a desktop system with an external neural stimulator (these results are beyond the

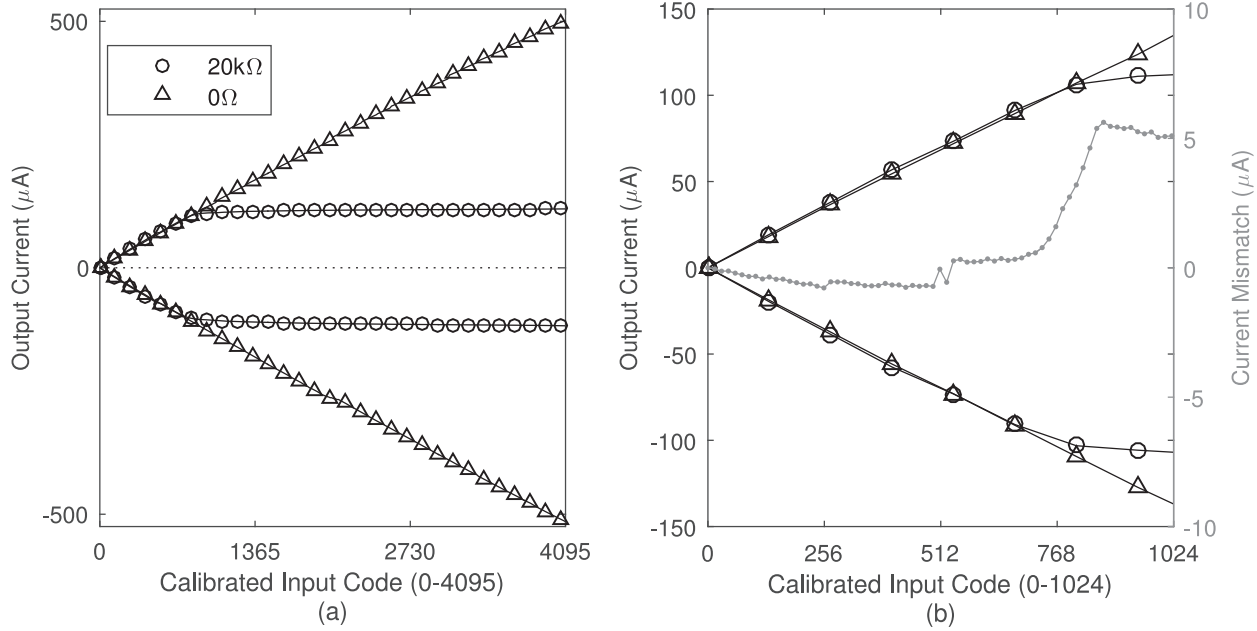


Fig. 6. Stimulation sweep over the entire input range with  $0\ \Omega$  and  $20\text{ k}\Omega$  loads. The LPU was designed to have a maximum output current of  $500\ \mu\text{A}$ , however the maximum output voltage is limited to  $5\text{ V}$ . (a) The output current over the full input range over the two loads. (b) Expanded region of (a) which is the effective operation range for the ISMS electrode array impedance.

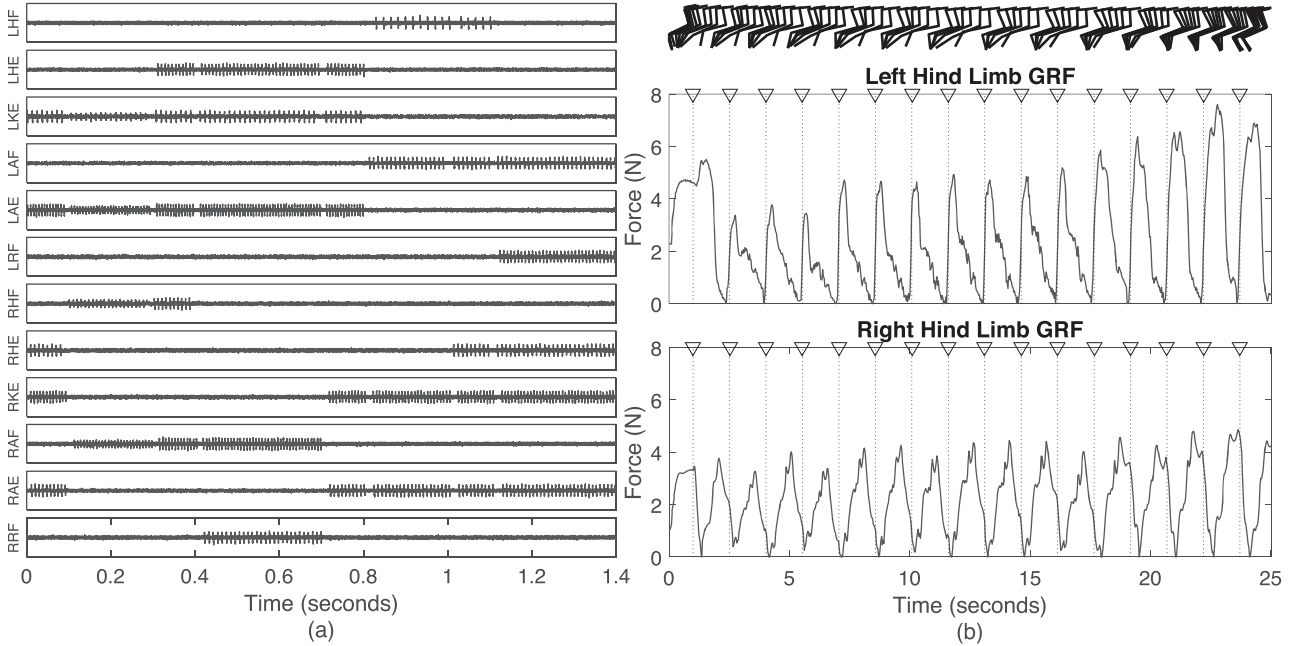


Fig. 7. Open loop operation using 8 states resembling those published in Mazurek *et al.* [25]. (a) Stimulation waveforms measured from the LPU for a 1.4 s walking period representing what was used during the *in-vivo* experiment. Each row corresponds to a stimulation channel activating left or right (L, R) hip, knee, or ankle (H,K,A) flexion or extension (F, E). For example, LHF stands for Left Hip Flexion. RF stands for rectus femoris which co-activates knee extension and hip flexion. Each channel has varying stimulation amplitudes for different state durations. (b) Ground reaction forces (GRFs) from one *in vivo* trial for the left and right hind limbs using an open-loop control strategy. Top trace depicts stick figure representation of the kinematic movements across the walkway. Bottom two traces depict GRFs from an open loop trial. Downward arrows and vertical dashed lines indicate the start of each stride where the stimulation pattern depicted in (a) would be implemented.

scope of this manuscript). The LPU produced movements and forces comparable to the desktop system used in the study. The design of the LPU provided for increased mobility for the delivery of ISMS since the device no longer required a constant connection to external hardware such as a desktop workstation or analog digitization board. The LPU produced 122 m of cu-

mulative over-ground walking across the 2.9 m walkway. Average supportive forces produced were comparable to that of the existing hardware system and produced functional walking in the setup (LPU:  $2.00 \pm 0.39\text{ N}$ , external system:  $1.68 \pm 0.35\text{ N}$ ). Kinematic and kinetic results from one trial are depicted in Fig. 7(b). The top trace shows a stick figure representation of

the right hind limb as it moved across the walkway. The bottom two traces represent the ground reaction forces (GRFs) for the left and right hind limbs. Upside down triangle markers and dashed lines indicate when the controller began each stride of the walking cycle. These markers correspond to when the stimulation patterns of Fig. 7(a) would occur during the trial. The forces produced for each limb were sufficient to propel the cat across the walkway. The left limb GRFs fluctuate more than the right limb which may be a result of the paw not landing consistently on the force plate during each step or the variable friction profile of the walkway itself.

The average power consumption of the device ( $P_{\text{avg}}$ ) was estimated using the average amount of power consumed in each state ( $P_{\text{stim}}$ ) and the amount of power consumed during state transitions ( $P_{\text{transition}}$ ). The implemented controller had a walking period of 1.5 s ( $T_{\text{stim}}$ ), and 8 state changes of duration 851.5  $\mu$ s ( $T_{\text{transition}}$ ) each. The maximal current each channel could output was 125  $\mu$ A (14 total channels) with a biphasic waveform duration of 490  $\mu$ s (two phases of 245  $\mu$ s each) at a frequency of 60 Hz. An average power consumption of 16 mW was consumed between state changes (as measured from a 5 V power supply). Assuming the maximal case scenario where all channels are active at their maximum current level for each state, the power consumption was estimated as: (see equation at the bottom of the page). This low power consumption is advantageous for a battery-powered device to last for long durations between recharging. More results from the full ISMS controlled walking study will be published in an upcoming manuscript.

## V. LPU IN SMALLER FABRICATION PROCESS

The results presented thus far demonstrate that the LPU fabricated in the ON Semiconductor 0.5  $\mu$ m produced walking forces and movements during an *in-vivo* experiment. Some limitations of the design were a result of insufficient space on the die to fit the necessary components. To address this, a second version of the LPU was fabricated in the IBM 0.18  $\mu$ m process to integrate more of the external components on chip (e.g., SRAM, analog switches, and bias voltages).

The 0.18  $\mu$ m version could only be powered to 3.3 V (compared to 5 V for the 0.5  $\mu$ m LPU), which was a limitation of the fabrication process. Using a symmetric stimulation waveform similar to the 0.5  $\mu$ m LPU would further reduce the effective operating range due to the output voltage compliance, with an estimated maximum stimulating current of 82.5  $\mu$ A. To increase the output current amplitude, this LPU version produced an asymmetric waveform (cathodic-leading) where the duration

of the anodic current was 10 times that of the cathodic current at 1/10th the amplitude [waveforms shown in Fig. 8(a)]. This allowed the cathodic stimulating current to reach the desired 125  $\mu$ A amplitude.

In this iteration of the LPU, a lower supply voltage (1.8 V) powered the digital circuitry to reduce power consumption from transient current as transistors turned on and off. On-chip SRAM cells were also implemented on chip to allow for quicker access to LPU parameters during operation and to load multiple parameters in parallel. The implemented SRAM cell was similar to the 6 transistor SRAM cell described in [48], but a voltage greater than the digital supply voltage was applied to the pass transistors to allow for a full logic ‘1’ to reduce excess leakage current [49]. To communicate between parts of the chip at different power levels, a level shifting circuit was used similar to that described in [50].

Bench tests for this LPU iteration demonstrate that it is capable of producing oscillating stimulation patterns using open loop control and closed loop control. A half-center oscillator (HCO) with two states was implemented such that one state stimulated while the other remained inactive and vice-versa [Fig. 8(b)]. The states transitioned with timed and sensory rules as shown in Fig. 8(c). An external voltage signal (2V<sub>pp</sub>, -1.5V<sub>offset</sub>, 0.1 Hz) representing sensory feedback was used to drive the transition from state 0 to state 1 with a threshold set to -1.0 V. The timing rule caused a state change from 1 to 0 after 8 s. The bottom traces in Fig. 8(c) depict when each state is active and when transitions occur.

One final bench test of this device was to replicate the open loop walking patterns used in Fig. 9 which produced the walking movements with the 0.5  $\mu$ m LPU. Using an array of 20 k $\Omega$  resistors to emulate the electrode array, Fig. 9 demonstrates that the measured output of the channels is similar to that in Fig. 9 which controlled flexion and extension of the hips, knees, and ankles [14], [32]. The stimulation amplitudes of each channel varies across different states depending on the desired movement response. The strength of the motor response increases with increasing stimulation levels, however, it is important to ensure the amplitude does not exceed the safety levels described by Cogan to prevent tissue damage [47]. This represents preliminary bench tests of the device but future work would need to verify its efficacy *in-vivo*.

## VI. DISCUSSION

These results demonstrate how the LPU can realize state-based systems for producing temporally adapting stimulation patterns. For restoring walking, the outputs displayed in

$$\begin{aligned} P_{\text{avg}} &= \frac{P_{\text{stim}} \times T_{\text{stim}} + P_{\text{transition}} \times T_{\text{transition}}}{T_{\text{stim}} + N_{\text{transitions}} \times T_{\text{transition}}} \\ &= \frac{5 [1.5 \text{ s} \times 60 \text{ Hz} \times 490 \mu\text{s} \times 125 \mu\text{A} \times 14 + 8 \times 851.5 \mu\text{s} \times 16 \text{ mA}]}{1.5 \text{ s} + 8 \times 851.5 \mu\text{s}} \\ &= 0.62 \text{ mW} \end{aligned}$$

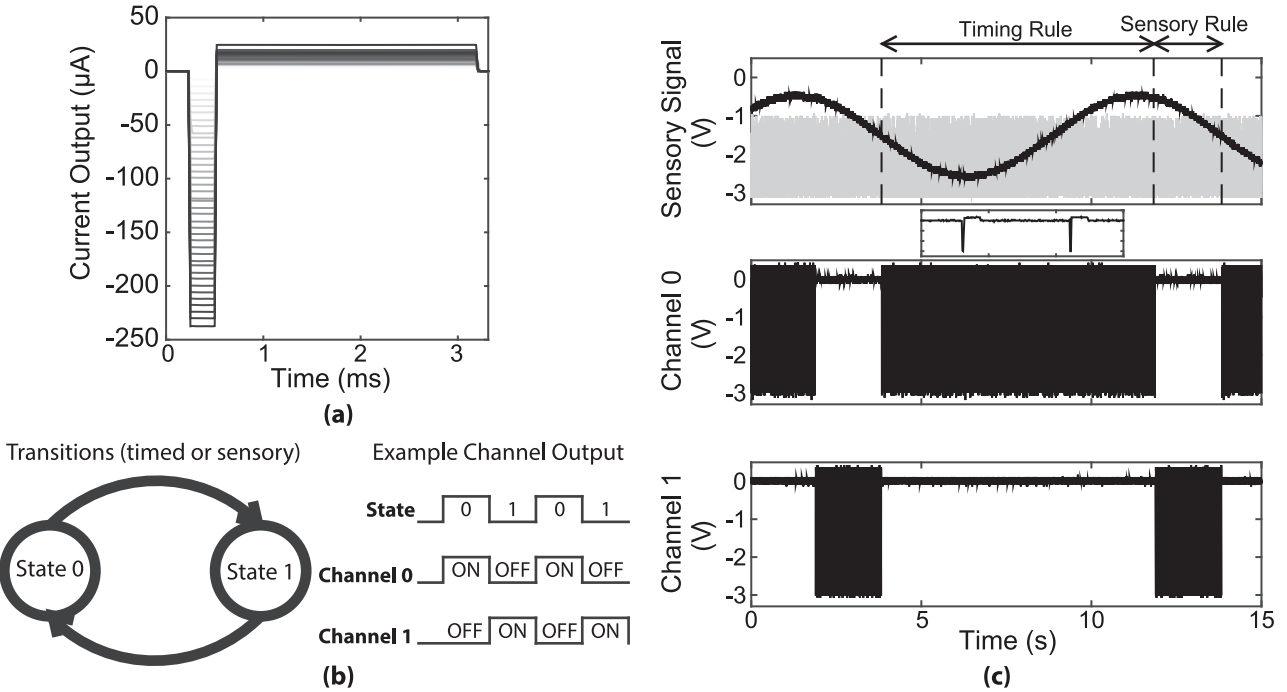


Fig. 8. (a) Asymmetric waveforms measured from the IBM 0.18  $\mu\text{m}$  LPU. (b) Schematic of the half-center oscillator which was programmed to demonstrate the ability to perform timed or sensory based state transitions. (c) Measurements from the HCO implemented on 2 states and 2 channels. The timing rule transitions from channel 0 to channel 1 and the sensory rule transitions from channel 1 to channel 0. The gray region in the top trace represents the voltage DAC output used for the sensory rule.

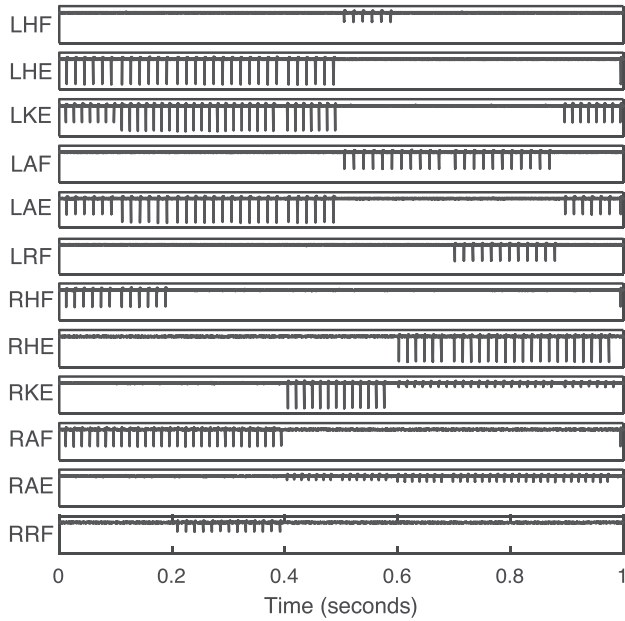


Fig. 9. Measured open loop stimulating outputs of the 0.18  $\mu\text{m}$  LPU measured over a 20  $\text{k}\Omega$  load. The walking period was set to 1 s and the state transitions are comparable to that demonstrated by the 0.5  $\mu\text{m}$  LPU. Future *in vivo* experiments would be needed to test the efficacy of this LPU version.

Fig. 11 match those conducted *in vivo* using open loop control in Mazurek *et al.* [32]. This device provides a reconfigurable platform for realizing different control strategies with the appropriate state transition rules and sensory inputs.

The architecture of the LPU produces programmable current stimulation outputs in parallel while temporally modulating the

activity using external sensory signals along with an internal timing signal. The configurability of the LPU provides the experimenter with resources to produce different walking “programs” which could potentially implement different modes of locomotion (e.g., running, walking, standing, hopping, etc.). Most existing microcontrollers or microprocessors have the ability to implement the designed control strategy, however they are limited in the number of DACs and ADCs on chip for digitizing the external analog sensors and producing current stimulation. As of this writing, two microprocessors which come close are designed by Analog Devices (Analog Devices, Norwood, MA, USA): ADUCM320 and ADUCM7122. These devices have between 13 and 16 ADCs for digitizing external signals. However, they only have 8 or 12 DACs for stimulating which is insufficient for this ISMS application. Additionally, the power consumption for these ICs are listed as 120 mW and 132 mW, respectively, exceeding the measured power consumption of the LPU (0.62 mW).

These and most other comparable microcontrollers are limited by their power supply range (3–3.6 V) which would result in needing an asymmetric stimulation waveform similar to the designed 0.18  $\mu\text{m}$  LPU. Future microprocessors may eventually have the desired number of ADCs and DACs for the current ISMS experimental setup, but one other limitation is that they will have to implement the stimulation output in a serial fashion by scanning from output electrode to output electrode. By using an array of integrate and fire neurons, the LPU is capable of producing the stimulation patterns in parallel and asynchronously from the control logic state machine. This allows for removing any delay times in the control logic from affecting the neural stimulation patterns.

For mobile applications, it is ideal for the hardware to operate for long durations between recharging and have a small physical footprint. This is the case when describing devices for use during walking. Many state of the art exoskeletal systems require carrying batteries to charge the system and can be considered bulky to maneuver. The *in vivo* performance of the first version of the LPU suggests that it can be integrated in future experimental designs. Recent work by Holinski *et al.* has demonstrated that it is possible to record from the dorsal root ganglia (DRG) to control the walking pattern produced using ISMS [51]. Their results use a similar state based control strategy which could be incorporated into the LPU platform to provide a system operating based on neural signals rather than external sensors (such as accelerometers or gyroscopes).

As the reproducibility and reduced variability of the ISMS implant improves, the limiting factor for a successful implantable device rests on the robustness of the control strategy itself. This will require a controller that is capable of responding to a wide range of perturbations outside of what is experienced in a laboratory environment. The advantage of housing the control strategy on the same die as the stimulators is that it allows for parallel operation of the controller and stimulators thus preventing potential bottlenecks in communication between the two. Future work will continue to improve the control performance as well as transition the device into an implantable package for mobile use.

## REFERENCES

- [1] L. R. Hochberg *et al.*, “Neuronal ensemble control of prosthetic devices by a human with tetraplegia,” *Nature*, vol. 442, pp. 164–171, Jul. 13, 2006.
- [2] J. M. Carmena *et al.*, “Learning to control a brain-machine interface for reaching and grasping by primates,” *PLoS Biol.*, vol. 1, p. E42, Nov. 2003.
- [3] F. V. Tenore, A. Ramos, A. Fahmy, S. Acharya, R. Etienne-Cummings, and N. V. Thakor, “Decoding of individuated finger movements using surface electromyography,” *IEEE Trans. Biomed. Eng.*, vol. 56, pp. 1427–1434, May 2009.
- [4] R. B. Stein, P. H. Peckham, and D. Popović, *Neural Prostheses: Replacing Motor Function After Disease or Disability*. Oxford, U.K.: Oxford Univ. Press, 1992.
- [5] V. K. Mushahwar, D. F. Collins, and A. Prochazka, “Spinal cord microstimulation generates functional limb movements in chronically implanted cats,” *Exp. Neurol.*, vol. 163, pp. 422–429, Jun. 2000.
- [6] V. K. Mushahwar and K. W. Horch, “Selective activation of muscle groups in the feline hindlimb through electrical microstimulation of the ventral lumbo-sacral spinal cord,” *IEEE Trans. Rehabil. Eng.*, vol. 8, pp. 11–21, Mar. 2000.
- [7] V. K. Mushahwar and K. W. Horch, “Muscle recruitment through electrical stimulation of the lumbo-sacral spinal cord,” *IEEE Trans. Rehabil. Eng.*, vol. 8, pp. 22–29, Mar. 2000.
- [8] J. A. Bamford, K. G. Todd, and V. K. Mushahwar, “The effects of intraspinal microstimulation on spinal cord tissue in the rat,” *Biomaterials*, vol. 31, pp. 5552–5563, Jul. 2010.
- [9] J. Gothe, S. A. Brandt, K. Irlbacher, S. Roricht, B. A. Sabel, and B. U. Meyer, “Changes in visual cortex excitability in blind subjects as demonstrated by transcranial magnetic stimulation,” *Brain*, vol. 125, pp. 479–490, Mar. 2002.
- [10] M. S. Graziano, C. S. Taylor, and T. Moore, “Complex movements evoked by microstimulation of precentral cortex,” *Neuron*, vol. 34, pp. 841–851, May 30, 2002.
- [11] B. Lau, L. Guevremont, and V. K. Mushahwar, “Strategies for generating prolonged functional standing using intramuscular stimulation or intraspinal microstimulation,” *IEEE Trans. Neural. Syst. Rehabil. Eng.*, vol. 15, pp. 273–285, Jun. 2007.
- [12] E. M. Schmidt, M. J. Bak, F. T. Hambrecht, C. V. Kufta, D. K. O’Rourke, and P. Vallabhanath, “Feasibility of a visual prosthesis for the blind based on intracortical microstimulation of the visual cortex,” *Brain*, vol. 119, pt. (Pt 2), pp. 507–522, Apr. 1996.
- [13] K. Deisseroth, “Optogenetics,” *Nat. Methods*, vol. 8, pp. 26–29, Jan. 2011.
- [14] B. J. Holinski, K. A. Mazurek, D. G. Everaert, R. B. Stein, and V. K. Mushahwar, “Restoring stepping after spinal cord injury using intraspinal microstimulation and novel control strategies,” in *Proc. IEEE Annu. Int. Conf. Engineering in Medicine and Biology Soc.*, 2011, pp. 5798–5801.
- [15] N. S. C. I. S. Center, *Spinal Cord Injury. Facts and Figures at a Glance*. Univ. Alabama Birmingham, Birmingham, AL, USA, 2013.
- [16] J. A. Blaya and H. Herr, “Adaptive control of a variable-impedance ankle-foot orthosis to assist drop-foot gait,” *IEEE Trans. Neural. Syst. Rehabil. Eng.*, vol. 12, pp. 24–31, Mar. 2004.
- [17] Neurotronics, The WalkAide System [Online]. Available: <http://www.walkwaide.com>.
- [18] D. J. Weber *et al.*, “BIONic WalkAide for correcting foot drop,” *IEEE Trans. Neural. Syst. Rehabil. Eng.*, vol. 13, pp. 242–246, Jun. 2005.
- [19] L. Mertz, “The next generation of exoskeletons: Lighter, cheaper devices are in the works,” *Pulse, IEEE*, vol. 3, pp. 56–61, 2012.
- [20] A. Tsukahara, R. Kawanishi, Y. Hasegawa, and Y. Sankai, “Sit-to-stand and stand-to-sit transfer support for complete paraplegic patients with robot suit HAL,” *Adv. Robotics*, vol. 24, pp. 1615–1638, 2010.
- [21] J. L. Contreras-Vidal and R. G. Grossman, “NeuroRex: A clinical neural interface roadmap for EEG-based brain machine interfaces to a lower body robotic exoskeleton,” in *Proc. 35th Annu. Int. Conf. IEEE Engineering in Medicine and Biology Soc.*, 2013, pp. 1579–1582.
- [22] G. G. Naples, J. T. Mortimer, and T. Yuen, *Overview of Peripheral Nerve Electrode Design and Implantation*. Englewood Cliffs, NJ, USA: Prentice Hall, 1990.
- [23] A. Prochazka, “Comparison of natural and artificial control of movement,” *IEEE Trans. Rehabil. Eng.*, vol. 1, pp. 7–17, 1993.
- [24] M. Levy, J. Mizrahi, and Z. Susak, “Recruitment, force and fatigue characteristics of quadriceps muscles of paraplegics isometrically activated by surface functional electrical stimulation,” *J. Biomed. Eng.*, vol. 12, pp. 150–156, Mar. 1990.
- [25] R. Kobetic, R. J. Triolo, and E. B. Marsolais, “Muscle selection and walking performance of multichannel FES systems for ambulation in paraplegia,” *IEEE Trans. Rehabil. Eng.*, vol. 5, pp. 23–29, Mar. 1997.
- [26] G. A. Tabot *et al.*, “Restoring the sense of touch with a prosthetic hand through a brain interface,” *Proc. Nat. Acad. Sci. USA*, vol. 110, pp. 18279–84, Nov. 5, 2013.
- [27] A. Kraskov, G. Prabhu, M. M. Quallo, R. N. Lemon, and T. Brochier, “Ventral premotor-motor cortex interactions in the macaque monkey during grasp: Response of single neurons to intracortical microstimulation,” *J. Neurosci.*, vol. 31, pp. 8812–8821, Jun. 15, 2011.
- [28] S. A. Overduin, A. d’Avella, J. M. Carmena, and E. Bizzi, “Microstimulation activates a handful of muscle synergies,” *Neuron*, vol. 76, pp. 1071–1077, Dec. 20, 2012.
- [29] R. Romo, A. Hernandez, and A. Zainos, “Neuronal correlates of a perceptual decision in ventral premotor cortex,” *Neuron*, vol. 41, pp. 165–173, Jan. 8, 2004.
- [30] M. C. Dadarlat, J. E. O’Doherty, and P. N. Sabes, “A learning-based approach to artificial sensory feedback leads to optimal integration,” *Nat. Neurosci.*, vol. 18, pp. 138–144, Jan. 2015.
- [31] L. Guevremont, J. A. Norton, and V. K. Mushahwar, “Physiologically based controller for generating overground locomotion using functional electrical stimulation,” *J. Neurophysiol.*, vol. 97, pp. 2499–2510, Mar. 2007.
- [32] K. A. Mazurek, B. J. Holinski, D. G. Everaert, R. B. Stein, R. Etienne-Cummings, and V. K. Mushahwar, “Feed forward and feedback control for over-ground locomotion in anaesthetized cats,” *J. Neural. Eng.*, vol. 9, p. 026003, Apr. 2012.
- [33] R. J. Vogelstein, F. Tenore, L. Guevremont, R. Etienne-Cummings, and V. K. Mushahwar, “A silicon central pattern generator controls locomotion *in vivo*,” *IEEE Trans. Biomed. Circuits Syst.*, vol. 2, pp. 212–222, Sep. 2008.
- [34] O. Ekeberg and K. Pearson, “Computer simulation of stepping in the hind legs of the cat: An examination of mechanisms regulating the stance-to-swing transition,” *J. Neurophysiol.*, vol. 94, pp. 4256–4268, Dec. 2005.

- [35] A. Prochazka, V. Gritsenko, and S. Yakovenko, "Sensory control of locomotion: Reflexes versus higher-level control," *Adv. Exp. Med. Biol.*, vol. 508, pp. 357–367, 2002.
- [36] K. Mazurek, B. Holinska, D. Everaert, R. Stein, V. Mushahwar, and R. Etienne-Cummings, "Locomotion processing unit," in *Proc. IEEE Biomedical Circuits and Systems Conf.*, 2010, pp. 286–289.
- [37] K. A. Mazurek and R. Etienne-Cummings, "Implementation of functional components of the locomotion processing unit," in *Proc. IEEE Biomedical Circuits and Systems Conf.*, 2011, pp. 21–24.
- [38] G. E. Goslow, Jr., R. M. Reinking, and D. G. Stuart, "The cat step cycle: Hind limb joint angles and muscle lengths during unrestrained locomotion," *J. Morphol.*, vol. 141, pp. 1–41, Sep. 1973.
- [39] J. M. Halbertsma, "The stride cycle of the cat: The modelling of locomotion by computerized analysis of automatic recordings," *Acta Physiol. Scand. Suppl.*, vol. 521, pp. 1–75, 1983.
- [40] J. F. Yang and D. A. Winter, "Surface EMG profiles during different walking cadences in humans," *Electroencephalogr. Clin. Neurophysiol.*, vol. 60, pp. 485–491, Jun. 1985.
- [41] T. Delbrück and A. Van Schaik, "Bias current generators with wide dynamic range," *Anal. Integr. Circuits Signal Process.*, vol. 43, pp. 247–268, 2005.
- [42] R. Saigal, C. Renzi, and V. K. Mushahwar, "Intraspinal microstimulation generates functional movements after spinal-cord injury," *IEEE Trans. Neural. Syst. Rehabil. Eng.*, vol. 12, pp. 430–440, Dec. 2004.
- [43] S. Yakovenko, V. Mushahwar, V. VanderHorst, G. Holstege, and A. Prochazka, "Spatiotemporal activation of lumbosacral motoneurons in the locomotor step cycle," *J. Neurophysiol.*, vol. 87, pp. 1542–1553, Mar. 2002.
- [44] V. K. Mushahwar and K. W. Horch, "Selective activation of muscle groups in the feline hindlimb through electrical microstimulation of the ventral lumbo-sacral spinal cord," *IEEE Trans. Rehabil. Eng.*, vol. 8, pp. 11–21, 2000.
- [45] V. G. Vanderhorst and G. Holstege, "Organization of lumbosacral motoneuronal cell groups innervating hindlimb, pelvic floor, and axial muscles in the cat," *J. Comp. Neurol.*, vol. 382, pp. 46–76, May 26, 1997.
- [46] V. K. Mushahwar, D. M. Gillard, M. J. Gauthier, and A. Prochazka, "Intraspinal micro stimulation generates locomotor-like and feedback-controlled movements," *IEEE Trans. Neural. Syst. Rehabil. Eng.*, vol. 10, pp. 68–81, Mar. 2002.
- [47] S. F. Cogan, "Neural stimulation and recording electrodes," *Annu. Rev. Biomed. Eng.*, vol. 10, pp. 275–309, 2008.
- [48] R. J. Baker, *CMOS: Circuit Design, Layout, and Simulation*. Hoboken, NJ, USA: Wiley, 2011, vol. 18.
- [49] J. M. Rabaey, A. P. Chandrakasan, and B. Nikolic, "Designing memory and array structures," in *Digital Integrated Circuits: A Design Perspective*, 2nd ed. Englewood Cliffs, NJ, USA: Prentice Hall, 2003, vol. 2.
- [50] P. O. Pouliquen, "A ratioless and biasless static CMOS level shifter," in *Proc. IEEE Int. Symp. Circuits and Systems*, 2010, pp. 4097–4100.
- [51] B. J. Holinski, D. G. Everaert, V. K. Mushahwar, and R. B. Stein, "Real-time control of walking using recordings from dorsal root ganglia," *J. Neural. Eng.*, vol. 10, p. 056008, Oct. 2013.



**Kevin A. Mazurek** (S'10–M'15) received the B.S. degree in electrical engineering from Brown University, Providence, RI, USA, in 2008, and the M.S. and Ph.D. degrees in electrical and computer engineering from Johns Hopkins University, Baltimore, MD, USA, in 2010 and 2014, respectively.

During his doctoral work, he received the F31 Ruth L. Kirschstein NRSA Award for studying the application of electrical stimulation of neural circuits in the spinal cord for movement. Currently, he is a Postdoctoral Researcher in the Department of Neurology and Center for Visual Science, University of Rochester, Rochester, NY, USA. His research interests include developing rehabilitation systems for enhancing or restoring motor function, including neural stimulation design.



**Bradley J. Holinski** received the B.S. degree in electrical engineering and the Ph.D. degree in biomedical engineering from the University of Alberta, Edmonton, AB, Canada.

Currently, he is an engineering professional with an interest, passion, and education in biomedical devices that record, interpret, and modulate signals within the nervous system. He is the Lead Project Engineer in the GSK Bioelectronics research group, which is dedicated to bringing bioelectronic medicines to people.



**Dirk G. Everaert** received the B.Sc. degree in physical therapy and the Ph.D. degree in motor rehabilitation and physiotherapy from the University of Leuven, Leuven, Belgium.

He specialized in orthopedic physical therapy, more specifically, spinal manipulative therapy and research on paraspinal soft tissue biomechanics at Emory University, Atlanta, GA, USA. He did postdoctoral training in neurosciences with Jane Macpherson at Oregon Health Sciences University, Portland, OR, USA, and with

Dr. Richard Stein at the University of Alberta, Edmonton, AB, Canada. Currently, he is a Research Associate with Dr. Stein and Dr. Vivian K. Mushahwar at the University of Alberta. His research interests include spine biomechanics, surface functional electrical stimulation, and intraspinal microstimulation to restore walking after injury or disease of the central nervous system.



**Vivian K. Mushahwar** (M'97) received the B.S. degree in electrical engineering from Brigham Young University, Provo, UT, USA, in 1991, and the Ph.D. degree in bioengineering from the University of Utah, Salt Lake City, UT, USA, in 1996.

She was a Postdoctoral Researcher at Emory University, Atlanta, GA, USA, and the University of Alberta, Edmonton, AB, Canada. Currently, she is a Professor in the Division of Physical Medicine and Rehabilitation, Department of Medicine and Centre for Neuroscience, University of Alberta. Her

research interests include identification of spinal cord systems involved in locomotion, development of spinal-cord-based neuroprostheses, incorporation of motor control concepts in functional electrical stimulation applications, and development of systems for alleviating secondary complications of immobility such as pressure ulcers and deep vein thromboses.

Dr. Mushahwar is a member of the International Functional Electrical Stimulation Society, the New York Academy of Sciences, the American Physiological Society, the International Society for Magnetic Resonance in Medicine, and the Society for Neuroscience.



**Ralph Etienne-Cummings** (F'13) received the B.S. degree in physics from Lincoln University, Lincoln, PA, USA, in 1988, and the M.S.E.E. and Ph.D. degrees in electrical engineering from the University of Pennsylvania, Philadelphia, PA, USA, in 1991 and 1994, respectively.

Currently, he is a Professor and Chairman of the Department of Electrical and Computer Engineering, Johns Hopkins University, Baltimore, MD, USA. He was the founding Director of the Institute of Neuro-morphic Engineering. He has authored more than 220 peer-reviewed articles, 11 books/chapters, and holds 10 patents/applications on his work.

Dr. Etienne-Cummings has served as Chairman of various IEEE Circuits and Systems (CAS) Technical Committees and was elected as a member of CAS Board of Governors. He also serves on numerous editorial boards. He is the recipient of the NSF's Career and Office of Naval Research Young Investigator Program Awards. He was a Visiting African Fellow at the University of Cape Town, Fulbright Fellowship Grantee, Eminent Visiting Scholar at the University of Western Sydney, and has won numerous publication awards, most recently the 2012 Most Outstanding Paper of the IEEE TRANSACTIONS ON NEURAL SYSTEMS AND REHABILITATION ENGINEERING. He was also recently recognized as a "ScienceMaker," an African American history archive.